ELSEVIER

Journal of Chromatography A, 762 (1997) 135–146

JOURNAL OF CHROMATOGRAPHY A

Effect of skeleton size on the performance of octadecylsilylated continuous porous silica columns in reversed-phase liquid chromatography

Hiroyoshi Minakuchi[a], Kazuki Nakanishi[a], Naohiro Soga[a], Norio Ishizuka[b], Nobuo Tanaka[b,*]

[a]*Kyoto University, Division of Material Chemistry, Faculty of Engineering, Yoshida, Sakyo-ku, Kyoto 606-01, Japan*
[b]*Kyoto Institute of Technology, Department of Polymer Science and Engineering, Matsugasaki, Sakyo-ku, Kyoto 606, Japan*

Abstract

We prepared continuous porous silica rods that had silica skeletons with sizes of 1.0–1.7 μm and through-pores of 1.5–1.8 μm, and evaluated their performance as a column in reversed-phase liquid chromatography. The mesoporous silica monoliths (mesopore size: 14 or 24 nm) were derivatized to C_{18} phase by on-column reaction with octadecyldimethyl-N,N-diethylaminosilane. The C_{18} silica rods gave minimum plate heights of 10–15 μm for aromatic hydrocarbons in 80% methanol and of 20–30 μm for insulin in acetonitrile–water mixtures in the presence of trifluoroacetic acid. The performance of the silica rods at a high flow-rate was much better than that of conventional columns packed with 5 μm C_{18} silica particles with pores of 12 or 30 nm, especially for high-molecular-mass species. Silica rods with the smaller sized silica skeletons resulted in Van Deemter plots showing a minimum plate height at the higher linear velocity of the mobile phase and a smaller dependence of plate height on the linear velocity. Separation impedance of less than 1000 was achieved with the continuous silica columns. The higher performance and lower pressure drop of silica rods at high flow-rates compared with particle-packed columns is provided by the small silica skeletons and large through-pores.

Keywords: Silica rods; Stationary phases, LC; Alkylbenzenes; Insulin

1. Introduction

In the course of the development of high-performance columns for high-performance liquid chromatography (HPLC) in 1970–1980, particles of smaller sizes were employed to obtain lower solvent consumption, shorter analysis times and better detectability, by generating larger numbers of theoretical plates per unit column length. Smaller particles can provide better column efficiency, based on the smaller eddy diffusion and shorter diffusion path length. Thus, the size of totally porous particles was reduced to 10 μm and then to 5 μm by the end of 1970s [1]. Silica particles with sizes of 1.5–2 μm have become available recently [2,3]. However, 5 μm particles are still the most widely used in HPLC today. The use of conventional columns packed with particles smaller than 3 μm has been limited, because of a high pressure drop associated with such particles. In most cases, these small particles are packed in relatively short columns, providing limited numbers of theoretical plates than can be generated with a longer column packed with 5 μm particles. Larger numbers of theoretical plates per unit time

*Corresponding author

PII S0021-9673(96)00944-2

can be obtained by using small particles under high pressure [4,5]. Most users, however, do not have the freedom to choose the pressure limit of the pump, the diameter of particles and the length of columns, beyond commercial availability.

The current limitation is due to the compromise between column efficiency and pressure drop. Independent control of the size of particles and the size of the interstitial void volume is not possible with conventional particle-packed columns. The use of pellicular-type packing materials and operation at high temperature were advocated to further increase the performance of particle-packed columns for high-molecular-mass solutes [6,7]. In open tubular chromatography, which can attain high efficiency at a low pressure drop, polymer coating of the tubing surface has been studied, leading to increased versatility [8,9]. More recently, capillary electrochromatography has been shown to be a promising approach for fully using the high performance of small particles [10–14].

Another approach to overcome the problem of a high column pressure drop associated with small particles is the use of a column made of one piece of a porous solid. Porous solid columns can show high performance at relatively low pressure, if they can be prepared to have small-sized skeletons and relatively large through-pores. The use of such a column, consisting of continuous porous polymers, has been reported recently [15–23]. Hjertén and coworkers [15,18], Li et al. [20], Svec and Frechet [17] and Wang et al. [19] showed high-speed separation of polypeptides with polymer rods in reversed-phase liquid chromatography (RPLC) and in ion-exchange chromatography. The performance of polymer rod columns has also been tested for small molecules in a few cases. Advantages of rod-type columns over conventional columns, however, have not been realized in isocratic elution of small molecules [21,22]. It would be of much interest to develop silica rod columns, because polymer-based HPLC packing materials usually possess micropores that result in a decrease in efficiency for small molecules [24,25].

Nakanishi et al. [26–28] reported the preparation of porous silica rods (monoliths) prepared by hydrolytic polymerization of tetramethoxysilane in the presence of water-soluble organic polymers. The silica rod possesses biporous structures, typically consisting of 0.3–5 μm silica skeletons, 0.5–8 μm through-pores, and 2–30 nm mesopores in the skeleton. In a preliminary report [29], we showed much better performance of such a continuous porous silica column having 1 μm silica skeletons and 1.7 μm through-pores, especially for a high-molecular-mass solute, than columns packed with 5 μm particles. The silica rod column also had a lower pressure drop due to higher permeability. Rod-type columns with small skeletons and relatively large through-pores may realize a high-efficiency separation at high speed, which is not possible with conventional particle-packed columns. We report here, in detail, the effect of skeleton size on the performance of octadecylsilylated (C_{18}) porous silica rods with relatively constant through-pore sizes.

2. Experimental

Silica rods were prepared following the procedure described previously [26–28]. Tetramethoxysilane (TMOS) was added to a solution of poly(ethylene oxide) (PEO: molecular mass=10 000; Aldrich, Milwaukee, WI, USA) in 0.01 *M* acetic acid (100 ml) and stirred at 0°C for 30 min. The composition of the reaction mixture was varied as shown in Table 1 so that silica rods [SR-(I) to SR-(IV)] with similar through-pore sizes and varied skeleton sizes were produced. The resulting mixture was poured into a polycarbonate mold (20 cm×9 mm I.D.) and allowed to react overnight at 40°C. Silica rods thus formed were washed with water, then treated with aqueous ammonium hydroxide solution (0.01 or 1.0 *M*) prior to acidification with aqueous nitric acid and a wash with 25% ethanol in water. After drying at 50°C for three days, the rods were treated at 600°C for 2 h and then were cut to the desired length.

We examined two series of silica rods (8.3 cm× 7.0 mm I.D.), with small (S: ca. 14 nm) or large (L: ca. 24 nm) mesopores, in this study, with different skeleton sizes designated as SR-(I) to SR-(IV) in Table 1, all having 1.5–1.8 μm through-pores. The 1.0 μm silica skeletons with 14 nm (S) or 24 nm (L) mesopores possess surface areas of ca. 370 (S) and 170 m^2/g (L), respectively. Columns were prepared

Table 1
Compositions of the preparation mixtures, the concentration of ammonium hydroxide and the pore properties of the produced silica rods

Silica rod No.	Composition[a]		NH_4OH[b] (mol/l)	Mesopore size[c] (nm)	Skeleton size[d] (μm)	Through-pore size[e] (μm)
	PEO (g)	TMOS (ml)				
SR-(I)-L	11.6	40	1.0	24.9	0.97	1.66
SR-(I)-S	11.6	40	0.01	14.3	1.00	1.86
SR-(II)-L	10.2	45	1.0	23.2	1.12	1.68
SR-(II)-S	10.2	45	0.01	13.1	1.16	1.73
SR-(III)-L	8.8	50	1.0	25.5	1.41	1.64
SR-(III)-S	8.8	50	0.01	14.2	1.34	1.65
SR-(IV)-L	7.0	55	1.0	24.3	1.66	1.58
SR-(IV)-S	7.0	55	0.01	15.8	1.59	1.53

[a]The amount of PEO and TMOS added to 100 ml of 0.01 *M* aqueous acetic acid.
[b]Concentration of NH_4OH used for controlling mesopore size after the preparation of a silica rod.
[c]Nitrogen adsorption.
[d]Estimated from the scanning electron micrographs by taking the average thickness of narrow (saddle) portions between branching points.
[e]Mercury porosimetry.

by encasing the silica rods in heat-shrinking poly(tetrafluoroethylene) (PTFE) tubing (Gunze electric insulation tubing, Gunze, Shiga, Japan) and PTFE column end-fittings and were used in a Z-module (Waters, Milford, MA, USA), which can apply an external pressure of up to 200 kg/cm^2 to the rod column. Chemical bonding of silica rods was carried out by applying a toluene solution of octadecyldimethyl-N,N-diethylaminosilane at 60°C to produce C_{18} phase, followed by trimethylsilylation with hexamethyldisilazane, as previously described [29,30].

Silica particles, Develosil (pore size, 11 nm; surface area, 330 m^2/g; Nomura Chem., Seto, Japan), and ordinary columns (15 cm×4.6 mm I.D.) packed with 5 μm silica C_{18} particles were obtained from commercial sources; Capcellpak C_{18} UG (pore size, 12 nm; Shiseido, Tokyo, Japan), Capcellpak C_{18} SG (pore size, 30 nm; Shiseido), Deltabond ODS (pore size, 30 nm; Keystone Scientific, Bellefonte, PA, USA) and Cosmosil MS-C_{18} (pore size, 11 nm; Nacalai Tesque, Kyoto, Japan). The mobile phase was prepared from LC-grade solvents. Insulin (bovine pancreas) was obtained from Sigma (St. Louis, MO, USA). Chromatographic measurement was carried out at 30°C. Size-exclusion chromatography (SEC) was carried out using a polystyrene standard and alkylbenzenes in tetrahydrofuran.

3. Results and discussion

3.1. Internal structures of continuous silica columns

Fig. 1 shows the internal structures of two silica rods, SR-(II)-S and SR-(IV)-S. The fractured surfaces show the silica skeletons of different sizes and through-pores penetrating several layers of these skeletons. In a conventional packed column, flow paths are provided as the interstitial voids between spherical particles having high tortuosity, because the particles must be tightly packed to produce high efficiency and stability of the packed bed. Although a close packing structure is not attained, the size of the particles determines the size of the interstitial voids in a packed column. Internal structures of packed columns of spherical particles with irregular interstices are represented by a touching sphere model [31].

In contrast, the size of through-pores in the silica rods can be controlled independently from the size of skeletons. They are relatively round and straight compared to the irregular shape of interstitial voids in packed columns. The preparation method of porous silica rods is known to produce a network structure of minimized surface areas [26,27]. Fig. 2 shows the size distribution of through-pores mea-

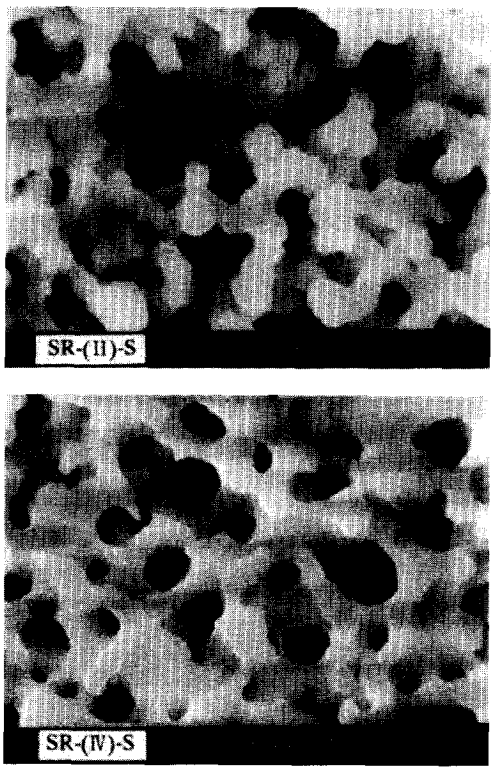

Fig. 1. Scanning electron micrograph of porous silica rods, SR-(II)-S and SR-(IV)-S.

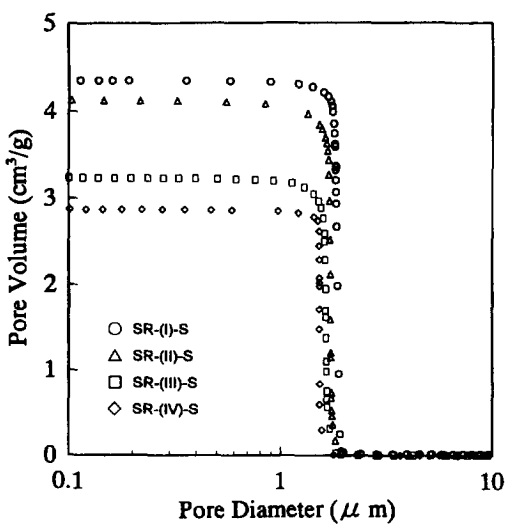

Fig. 2. Pore size distribution of silica rods measured by mercury intrusion with SR-(I)-S (○), SR-(II)-S (△), SR-(III)-S (□) and SR-(IV)-S (◇).

sured by mercury porosimetry. The results show narrower size distributions compared with the interstitial voids in packed columns [31,32]. The through-pore size of about 1.5–1.8 μm should be similar to the size of interstitial voids in a conventional column packed with 5 μm spherical particles. The size of the interstitial voids in a column packed with spheres has been shown to be 25–40% of the particle's size [31–33].

Table 1 lists the pore sizes of continuous silica rods. The sizes of through-pores and mesopores remained relatively constant under the preparation conditions. The treatment with 0.01 *M* aqueous ammonia during the preparation produced SR-S with 14 nm mesopores and a surface area of 370 m^2/g, which is somewhat greater than those of silicas with similar pore sizes that are usually employed as a support of the C_{18} phase. This may indicate the presence of small pores [29]. The treatment of a silica rod with ammonia of higher concentration (1.0 *M*) removed the micropores to produce SR-L, with 24 nm pores and a surface area of 170 m^2/g.

The skeleton sizes shown are the averaged thickness of narrow (saddle) portions between branching portions of skeletons on the scanning electron micrographs. A ratio of greater than unity between the size of the through-pores and the size of the skeleton of silica rods is much greater than those of ordinary columns packed with spherical particles [31–33]. As shown in Table 2, with a total porosity of 86% and an internal porosity of 21%, the volume of the through-pores accounts for 65% of the column volume in SR-(I)-S, which is greater than that found in conventional packed columns by about 25% [31,32]. The continuous silica column was shown to be more loosely occupied by a solid and to have a larger cross-sectional area of through-pores than conventional columns, resulting in lower flow resistance, as shown later.

3.2. Chemical modification of a continuous silica column

Chemical modification of silica rods was carried out by reacting alkylaminosilanes that are effective silylating reagents for on-column reaction [30]. Octadecylsilylation reduced the volume of the mesopores, resulting in 81% total porosity with SR-(I)-S-

Table 2
Volumes of through-pores and mesopores in silica rods and particle-packed columns.

Pore volume	Volume fraction of a column[a]				
	Silica rod SR-(I)-S		Particle-packed column		
			Develosil[b]		Capcellpak C_{18} UG
	Before ODS	After ODS	Before ODS	After ODS	
Total porosity	0.86	0.81	0.78	0.66	0.60
Through-pore[c]	0.65	0.65	0.39	0.39	0.32
Mesopore	0.21	0.16	0.40	0.27	0.29
Bonded phase	–	0.05	–	0.13	–
(Phase ratio)	–	(0.06)	–	(0.19)	–

[a]Measured by size-exclusion chromatography with total column volume as 1.0.
[b]Develosil (Nomura Chemicals, Seto, Japan; particle size, 5 μm; pore size, 11 nm).
[c]Interstitial void volume in the case of particle-packed column.

C_{18} compared to 66% in a C_{18} silica-packed column. The amount of alkyl groups per unit volume of a rod (5% of a column volume) is much smaller than that in a particle-packed column (12.5% of column volume). Accordingly, the phase ratio in SR-(I)-S-C_{18}, 5/81, is smaller than that in the particle-packed column, 12.5/66, by a factor of about three. While these phase ratios were estimated based on the results of SEC measurement in tetrahydrofuran, the comparison of phase ratios agreed with that in retention in reversed-phase mode. The k' values for aromatic hydrocarbons on SR-(I)-S-C_{18} in 80% methanol were about one third of those on a C_{18} phase prepared from silica particles of 11–12 nm mesopores (Table 3).

The surface coverage with the octadecylsilyl groups was nearly maximal, as estimated from a retention increase caused by one methylene group in 80% methanol [34], which indicates that the hydrophobic selectivities, $\alpha(CH_2)$, of SR-(I)-S-C_{18} and SR-(I)-L-C_{18} are similar to those of stationary phases commercially available. With the larger mesopores, lower $\alpha(CH_2)$ values were obtained. The retention ratio between solutes with different planarities, triphenylene (T) and *ortho*-terphenyl (O), with $\alpha(T/O)=1.52–1.55$ in 80% methanol also indicates a high surface coverage [34]. Repeated reactions with octadecyldimethyl-N,N-diethylaminosilane did not increase the retention significantly. Trimethylsilylation reduced the retention

Table 3
Retention and selectivity for hydrocarbons.

Column	Mesopore (nm)	k'[a] Amylbenzene	$\alpha(CH_2)$[b]	$\alpha(T/O)$[c]
SR-(I)-S-C_{18}	14	2.15	1.48	1.55
SR-(I)-L-C_{18}	25	1.07	1.46	1.52
Cosmosil C_{18} MS	11	6.33	1.51	1.44
Capcellpak C_{18} UG	12	5.58	1.49	1.38
Capcellpak C_{18} SG	30	2.58	1.47	1.44
Deltabond ODS 300	30	0.98	1.42	1.16

[a]The k' values of amylbenzene in 80% methanol.
[b]Separation factor (α) between amylbenzene and butylbenzene in 80% methanol.
[c]Separation factor (α) between triphenylene (T) and *ortho*-terphenyl (O) in 80% methanol.

of hydrogen-bond acceptors such as caffeine, reflecting the reduction of the number of accessible silanols.

3.3. Performance of C_{18} silica rods

Chromatographic performance of C_{18} silica rods was examined with the elution of alkylbenzenes in 80% methanol, and with insulin in acetonitrile–water mixtures in the presence of trifluoroacetic acid (TFA). Fig. 3 shows the comparison between SR-(I)-L-C_{18}, SR-(I)-S-C_{18} and Capcellpak C_{18} UG in the elution of alkylbenzenes. Although accompanied by slight tailing, the 83 mm rod produced about 6000–8000 theoretical plates, with a height equivalent to a theoretical plate (HETP) of ca. 10–14 μm, compared with Capcellpak UG (15 cm column), which generated 11 000 plates. The decrease in column efficiency at higher flow-rates is more obvious with a column packed with 5 μm C_{18} silica particles than with the silica rod columns. SR-(I)-L-C_{18} maintained 90% of the plate number at 5 mm/s compared to 1.5 mm/s, while up to a 50% reduction in plate number was observed with the particle-packed column.

The difference in performance at high speed between the rod-type columns and the particle-packed columns was more obvious for a solute with a higher molecular mass, as expected. Fig. 4 shows the comparison for insulin. The composition of acetonitrile–water mixtures was varied slightly, to

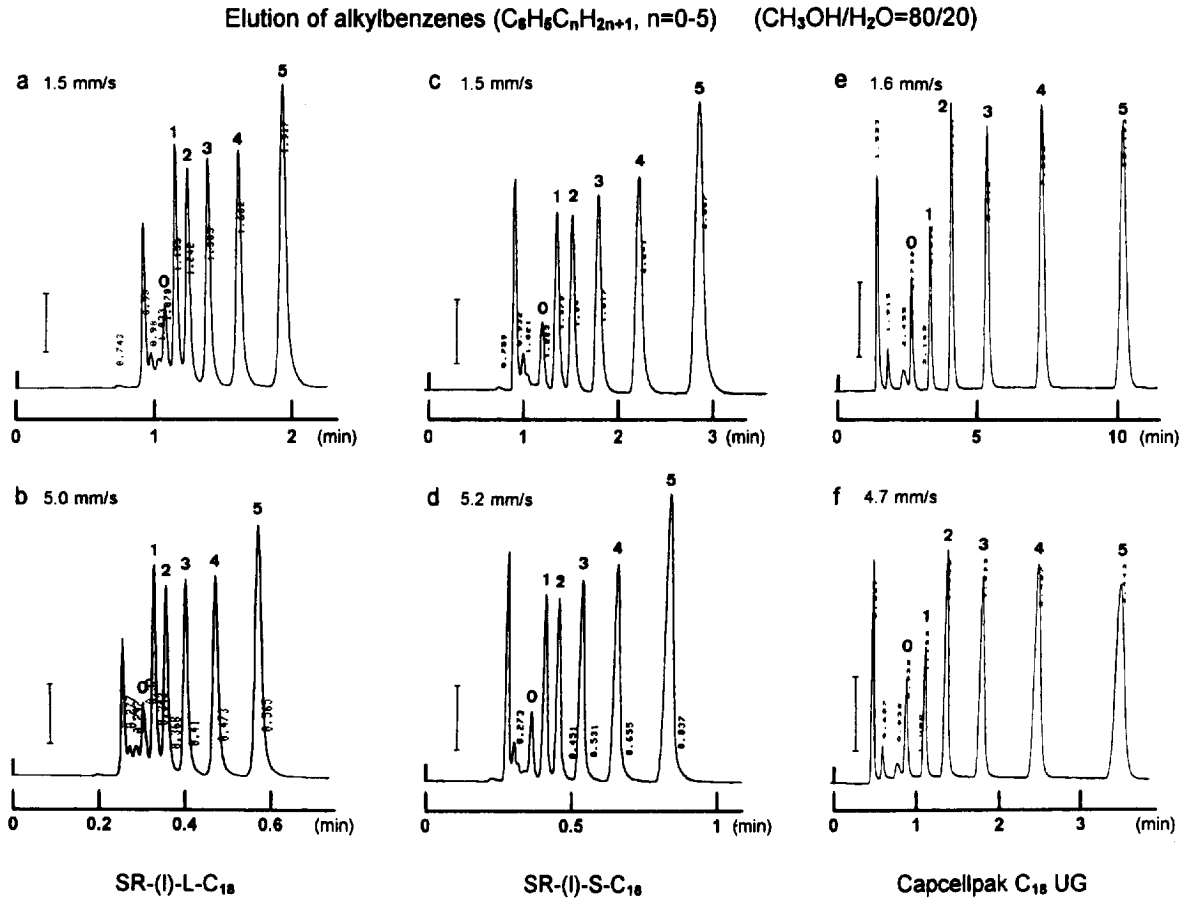

Fig. 3. Elution of alkylbenzenes ($C_6H_5C_nH_{2n+1}$, $n=0$–5) in 80% methanol on silica rod columns SR-(I)-L-C_{18} (a and b), SR-(I)-S-C_{18} (c and d) (column length, 8.3 cm) and on Capcellpak C_{18} UG (column length, 15 cm; e and f). Mobile phase linear velocity: 1.5 mm/s (a), 5.0 mm/s (b), 1.5 mm/s (c), 5.2 mm/s (d), 1.6 mm/s (e) and 4.7 mm/s (f). The scale bars indicate 0.05 AU at 215 nm.

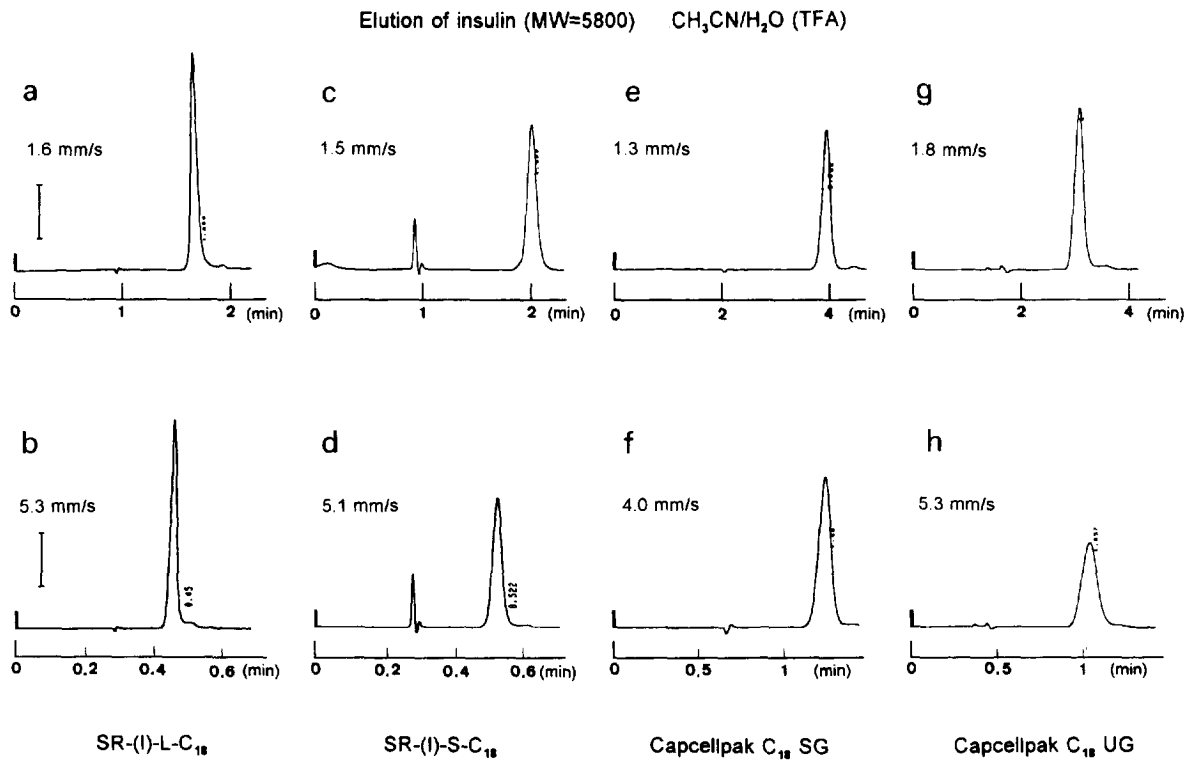

Fig. 4. Isocratic elution of insulin in acetonitrile–water mixtures in the presence of TFA. Column: SR-(I)-L-C_{18} (a and b), SR-(I)-S-C_{18} (c and d), Capcellpak C_{18} SG (e and f) and Capcellpak C_{18} UG (g and h). Mobile phase linear velocity: 1.6 mm/s (a), 5.3 mm/s (b), 1.5 mm/s (c), 5.1 mm/s (d), 1.3 mm/s (e), 4.0 mm/s (f), 1.8 mm/s (g) and 5.3 mm/s (h). Mobile phase: acetonitrile–water (30:70, v/v) for SR-(I)-S-C_{18}, 30:70 (v/v) for SR-(I)-L-C_{18}, 31.5:68.5 (v/v) for Capcellpak C_{18} UG (12 nm) and 32:68 (v/v) for Capcellpak C_{18} SG in the presence of 0.1% TFA. The scale bars indicate 0.05 AU at 215 nm in (a)–(h).

adjust k' values, because high-molecular-mass compounds are hard to elute with the same mobile phase composition from various stationary phases. Silica particles with 12 nm pores showed poor column efficiencies for insulin, especially at high flow-rates. Wide pore (30 nm) silica particles showed better column efficiency than small pore particles. Rod-type columns, particularly SR-(I)-L-C_{18}, showed better column efficiency for insulin than packed columns. At higher flow-rates, much greater differences were observed.

The Van Deemter plots obtained with amylbenzene as a solute in 80% methanol are shown in Fig. 5. A column packed with 5 μm particles gave a minimum plate height (H_{min}) of ca. 13 μm at a low flow-rate and a sharp increase in plate height (HETP) with an increase in linear velocity. Fig. 5 indicates that the performance of the C_{18} silica rods with 1.5–1.8 μm through-pores is similar to, or better than, that of columns packed with 5 μm particles. C_{18} silica rods generally provided H_{min} at higher linear velocity. The silica rods with 14 nm mesopores showed H_{min} of 12–14 μm, comparable with the H_{min} obtained with 5 μm Capcellpak C_{18} UG with 12 nm mesopores. Slightly higher H_{min} values were observed on SR-S-C_{18} than on SR-L-C_{18}. This may be due to the presence of small pores in SR-S-C_{18}.

The increase in HETP with flow-rate that was found with Capcellpak C_{18} SG and Deltabond ODS with 30 nm pores is smaller than that with Capcellpak C_{18} UG. The silica rods showed even smaller dependence of HETP on linear velocity. The effect of skeleton size is clearly observed. The smaller the skeleton size, the smaller the slope of the plots. This is understandable based on the diffusion path length. The dependency of HETP at high mobile phase

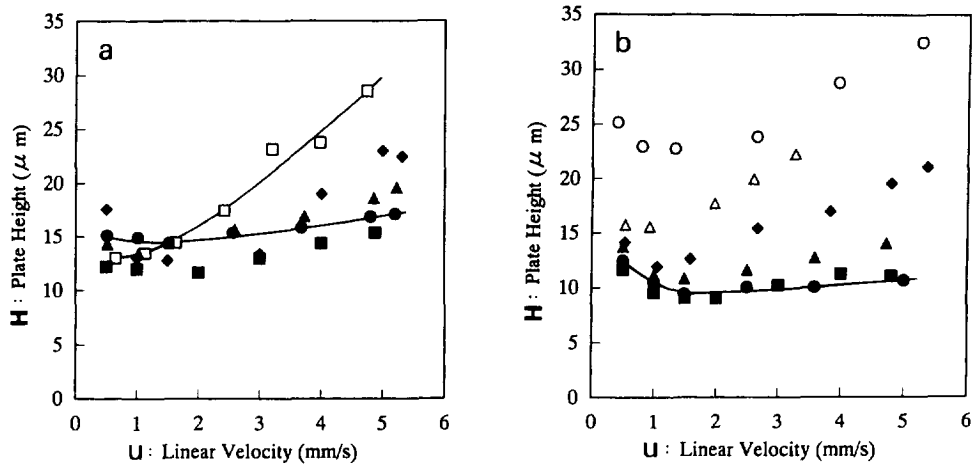

Fig. 5. Van Deemter plots for C_{18} silica rods and silica C_{18}-packed columns with amylbenzene as the solute. Mobile phase: 80% methanol. (a) ●, SR-(I)-S-C_{18}; ▲, SR-(II)-S-C_{18}; ■, SR-(III)-S-C_{18}; ♦, SR-(IV)-S-C_{18} and □, Capcellpak C_{18} UG (12 nm). (b) ●, SR-(I)-L-C_{18}; ▲, SR-(II)-L-C_{18}; ■, SR-(III)-L-C_{18}; ♦, SR-(IV)-L-C_{18}; ○, Capcellpak C_{18} SG (30 nm); △, Deltabond ODS (30 nm). Curves connect the plots for SR-(I)-S-C_{18}, SR-(I)-L-C_{18} and Capcellpak C_{18} UG.

linear velocity is dominated by a term proportional to the square of the particle size or the skeleton size [1,35]. SR-(I)-L-C_{18} resulted in an extremely flat curve, as reported with 2 μm particles [3]. Thus, all of the silica rods showed much smaller HETP values or much higher column efficiencies than the particle-packed columns at high linear velocity.

The Van Deemter plots obtained with insulin as a solute are shown in Fig. 6. For these measurements, the eluent strength was adjusted to give similar k' values for insulin on each column by changing the acetonitrile content by up to 3.5%. The wide-pore C_{18} silica particles showed lower plate heights and a smaller slope for insulin than particles having 12 nm pores. Fig. 6 shows that the column efficiencies of the C_{18} silica rods for insulin, with a molecular mass

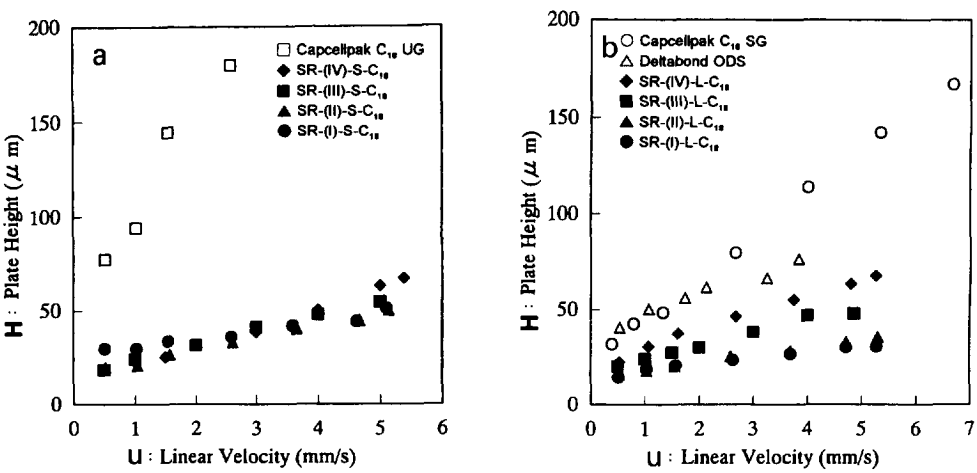

Fig. 6. Van Deemter plots for C_{18} silica rods and silica C_{18}-packed columns with insulin as the solute. Mobile phase: acetonitrile–water (33.5:66.5, v/v) for Deltabond ODS (30 nm) in the presence of TFA, and the other columns as in Fig. 4. (a) ●, SR-(I)-S-C_{18}; ▲, SR-(II)-S-C_{18}; ■, SR-(III)-S-C_{18}; ♦, SR-(IV)-S-C_{18} and □, Capcellpak C_{18} UG (12 nm). (b) ●, SR-(I)-L-C_{18}; ▲, SR-(II)-L-C_{18}; ●, SR-(III)-L-C_{18}; ♦, SR-(IV)-L-C_{18}; ○, Capcellpak C_{18} SG (30 nm) and △, Deltabond ODS (30 nm).

of ca. 5800, were much better than that of 5 μm C_{18} silica particles, especially at high flow-rates. A correlation between the skeleton size and the slope of the plots was clearly observed, as in Fig. 5. The silica rod, SR-(I)-L-C_{18}, with small skeletons and large mesopores, provided the best results. This is presumably due to the short diffusion path length associated with the small-sized skeletons of the silica rods. The small skeleton size may allow the use of rods with small mesopores for high-molecular-mass solutes, although 5 μm particles possessing small pores showed poor efficiencies for high-molecular-mass polypeptides compared with macroporous polymer-based packing materials [36]. High column efficiency at high speed has also been reported with polymer rod columns under gradient conditions [17–20].

$$H = \frac{1}{(1/C_e d_p) + [1/(C_m d_p^2 u/D_m)]} + \frac{C_d D_m}{u} + \frac{C_{sm} d_p^2 u}{D_m} \quad (1)$$

$$H = Au^{1/3} + B/u + Cu \quad (2)$$

$$h = A\nu^{1/3} + B/\nu + C\nu \quad (3)$$

$$h = H/d_p, \quad \nu = ud_p/D_m \quad (4)$$

A plate height (H) for a particle-packed column is described by Eq. (1) or Eq. (2) [35,37], where d_p is the particle diameter, u is the linear velocity of the mobile phase, D_m is the diffusion coefficient of the solute, C_e, C_m, C_d and C_{sm} are coefficients representing the contribution of eddy diffusion, mobile-phase mass transfer, longitudinal diffusion and mass transfer within a particle, respectively. The equation is also expressed in reduced parameters as in Eq. (3) [38], where h is a reduced plate height, and ν is a reduced velocity. The reduced velocity for insulin is much higher than for amylbenzene at the same linear velocity because of its smaller diffusion coefficient [39] and this is shown by the plots without H_{min} for insulin in Fig. 6.

In order to plot the data according to Eq. (3), an effective d_p for a silica rod is required in Eq. (4). The d_p is a particle diameter with a particle-packed column, and has been used when considering the C-term contribution within particles and the A-term contribution in the mobile phase as a unit length describing the distance for a molecule to diffuse or flow to change its velocity in the derivation of Eq. (1) [35], because the size of interstitial channels in a packed column is determined by the size of the particles to be about 1/3 of a particle diameter. In the case of a silica rod, it would be appropriate to take the sum of the through-pore size and the size of silica skeletons at narrow (saddle) portions to be d_p in Eq. (4). The sum of the sizes of through-pores and the narrow skeletons is the repeating unit size of domains in the preparation process of a silica rod involving phase separation [26,27]. Although it may be appropriate to take the size of branching portions of silica skeletons as being d_p, the sizes at these portions are hard to measure. Actually, the size of silica skeletons at these portions is not too far from the combined size of the domains. Because the size of through-pores relative to that of silica skeletons is controllable in a silica rod (and larger than in a packed column), the combined domain size would better represent the unit length when considering various flow and diffusional effects on band broadening in the mobile phase in a silica rod.

Fig. 7 shows the plots of log h against log ν for Capcellpak C_{18} SG, SR-(I)-L-C_{18} and SR-(IV)-L-C_{18}. The plots for Capcellpak are characterized by high h_{min} due to the high A term. The slight

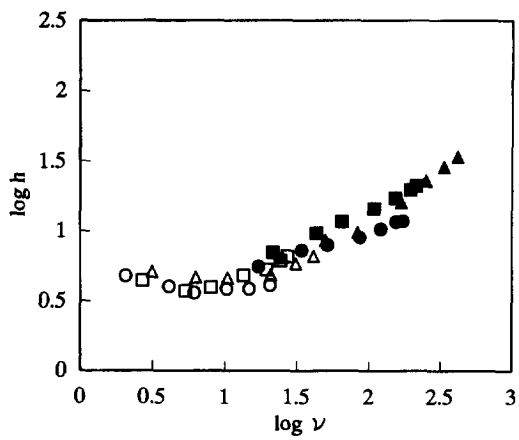

Fig. 7. Plots of log h against log ν with amylbenzene (open symbols) and insulin (closed symbols) as solutes on SR-(I)-L-C_{18} (○,●), SR-(IV)-L-C_{18} (□,■) and Capcellpak C_{18} SG (△,▲). See Figs. 5 and 6 for conditions.

discontinuity between the plots for amylbenzene and those for insulin seen with the silica rods can arise from errors in the calculated diffusion coefficients or from the presence of small pores that give poorer performance for a high-molecular-mass solute. Greater discontinuity was observed with the small-pore materials, Capcellpak C_{18} UG and SR-S-C_{18} rods. Estimation of values of A and C in Eq. (3) from the plots for insulin in Fig. 7 gave A values of 1.7, 2.1 and 2.1 for Capcellpak C_{18} SG, SR-(I)-L-C_{18} and SR-(IV)-L-C_{18}, and C values of 0.05, 0.001 and 0.02, respectively. Although the C value for SR-(I)-L-C_{18} seems to be underestimated by the present treatment, which assumes that h for insulin depends on $A\nu^{1/3}+C\nu$, the results suggest that the plots for the silica rods can be characterized by large A terms and small C terms. This tendency is also seen in Figs. 5 and 6. The relatively large contribution of the A term with silica rods can be explained by taking into account the presence of relatively large and straight through-pores. Solutes can be carried away much further without being mixed due to the low tortuosity, resulting in greater band broadening. In the case of particle-packed columns with higher tortuosity, more efficient mixing occurs to average the contribution of eddy diffusion or to make the step length shorter.

Small skeletons of silica rods in the presence of large through-pores allow fast equilibration even for large molecules, while the mesopores provide sample loading capacity, as in packing materials for perfusion chromatography [40,41]. The Knox plots in Fig. 7 show the better performance of the rod columns than of the perfusive packing materials, although the latter packed in capillary columns gave better results for unretained solutes [42]. The comparison also indicates the significant contribution that the A term makes with the silica rod columns.

Antia and Horváth [6] and Chen and Horváth [7] demonstrated that improved column efficiency was obtained by the use of pellicular packings at high temperatures [6,7], which also reduced the contribution of the diffusional effects and the pressure drop. Such an approach may, however, be associated with low sample loading capacity and some inconvenience related to high temperature operation, while porous silica rods can have good capacity and high performance at room temperature. These results clearly indicate the advantage of the rod-type columns over conventional particle-packed columns to achieve high-speed separations. Similar attempts have been reported with various polymer rods [15–23] and with porous glass rods with 2 μm through-pores and without mesopores [43].

3.4. Total column performance of continuous silica columns including pressure drop

The size of interstitial void spaces between spherical particles is commonly 25–40% of the size of particles [31–33]. Therefore, the size of interstitial openings in columns packed with 5 μm particles should be similar to those of the rods used in this study. The silica rods with through-pores of 1.5–1.8 μm, however, produced a much lower pressure drop than that produced by conventional columns packed with 5 μm particles, as shown in Fig. 8, where the column length was normalized. High column efficiency, together with the small pressure drop observed with the silica rods, is a significant advantage and can be explained by the small-sized skeletons surrounded by relatively large through-pores. The flow resistance factor (ϕ) calculated from

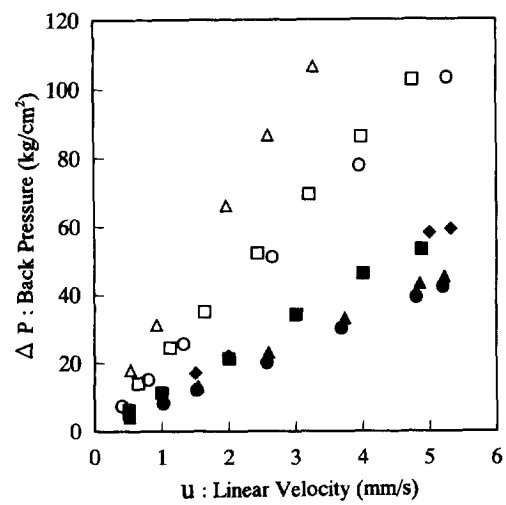

Fig. 8. Plots of column back pressure against linear velocity of mobile phase. Mobile phase: 80% methanol. The pressures were normalized to the column length of 83 mm. ●, SR-(I)-S-C_{18}; ▲, SR-(II)-S-C_{18}; ●, SR-(III)-S-C_{18}; ♦, SR-(IV)-S-C_{18}; □, Capcellpak C_{18} UG (12 nm); ○, Capcellpak C_{18} SG (30 nm) and △, Deltabond ODS (30 nm).

the external porosity using the Kozeny-Carman equation in combination with Darcy's law is 80–130 for the silica rods, assuming spherical skeletons, approximately an order of magnitude smaller than those of packed columns [1,38].

Pressure drop is an important parameter in determining the maximum number of theoretical plates obtainable per unit time. Normally, operation at a flow-rate that gives H_{min} is recommended [1,4,38]. Operation at high speed is not compatible with high efficiency in the case of particle-packed columns with larger-sized particles, due to a sharp increase in HETP, and is not possible with smaller-sized particles, either, due to a large pressure drop, limiting the number of theoretical plates of columns for routine applications.

$$E = \frac{\Delta P}{N} \cdot \frac{t_0}{N} \cdot \frac{1}{\eta} \quad (5)$$

The total performance of a column can be assessed based on the separation impedance given by Eq. (5) [38], which gives the E value as the product of the reciprocal number of theoretical plates per unit pressure drop, the reciprocal number of theoretical plates per unit time and the reciprocal mobile phase viscosity. The separation impedance (E), calculated for Capcellpak C_{18} UG at H_{min}, is approximately 3500, while E values of 800–900 were obtained with SR-(I)-L-C_{18} and SR-(III)-L-C_{18}. More significantly, the low separation impedance was obtained in the high linear velocity region, as shown in Fig. 9. This implies that it may be possible to produce high column efficiency per unit time while limiting the pressure.

In a practical example, let us suppose a column of 15 cm is operated at 1.5 mm/s to produce 12 500 plates ($H = 12$ μm) with a t_0 value of 100 s (retention time of 400 s at $k' = 3$). The pressure drop is about 30 kg/cm^2 for a silica rod column and about 60 kg/cm^2 for 5 μm particles in the mobile phase used for Figs. 3 and 5. It would be possible to get about three times as many theoretical plates within the same period of time with current instrumentation by using a silica rod column three times as long and a flow-rate that was as many times higher. This is impossible with 5 μm particle-packed columns for two reasons; the loss of column efficiency at high flow-rates and the high pressure drop (see Figs. 5 and 8).

In conclusion, silica rods having skeletons of 1–1.7 μm and 1.5–1.8 μm through-pores provided higher column efficiency at high speed and a smaller pressure drop than columns packed with 5 μm particles. The use of such continuous silica columns may lead to high efficiency and high speed sepa-

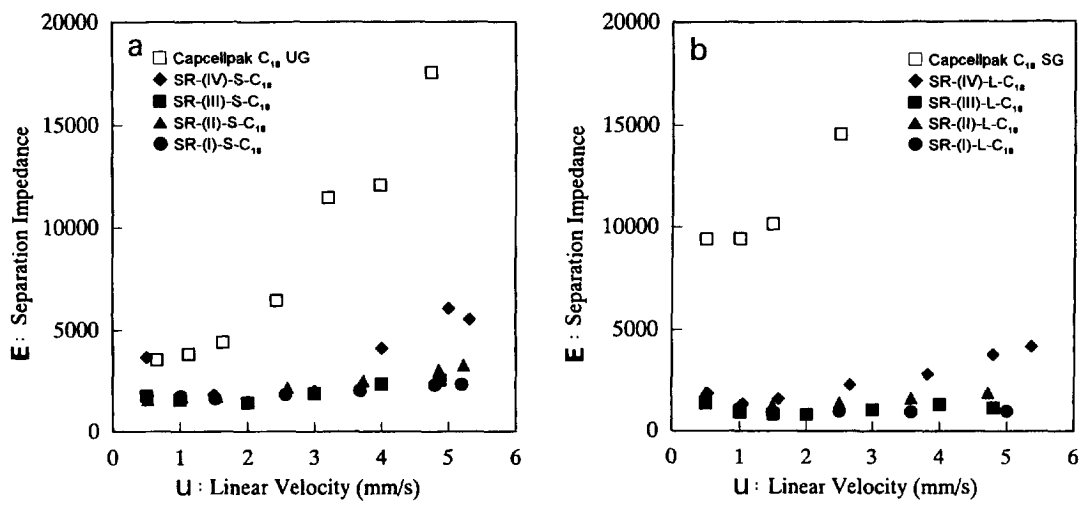

Fig. 9. Plots of separation impedance against linear velocity of mobile phase calculated for amylbenzene as the solute in 80% methanol. (a) ●, SR-(I)-S-C_{18}; ▲, SR-(II)-S-C_{18}; ■, SR-(III)-S-C_{18}; ♦, SR-(IV)-S-C_{18} and □, Capcellpak C_{18} UG (12 nm). (b) ●, SR-(I)-L-C_{18}; ▲, SR-(II)-L-C_{18}; ■, SR-(III)-L-C_{18}; ♦, SR-(IV)-L-C_{18} and ○, Capcellpak C_{18} SG (30 nm).

rations that are not possible with current particle-packed columns.

Acknowledgments

This work was supported in part by grant-in-aid for scientific research (No. 07555480) and the Monbusho International Joint Research Program (No. 07044084 and 08044079) funded by the Ministry of Education, Science, Sports, and Culture. The authors thank Dr. L.R. Snyder and Dr. J.W. Dolan for helpful comments. We also thank Masaya Mitani for technical assistance.

References

[1] G. Guiochon, in Cs. Horváth (Editor), High Performance Liquid Chromatography — Advances and Perspectives, Vol. 2, Academic Press, New York, 1980, pp. 1–56.
[2] K.K. Unger, G. Jilge, J.N. Kinkel and M.T.W. Hearn, J. Chromatogr., 359 (1986) 61–72.
[3] H. Moriyama, M. Anegayama, K. Komiya and Y. Kato, J. Chromatogr. A, 691 (1995) 81–89.
[4] J.H. Knox, J. Chromatogr. Sci., 15 (1977) 352–364.
[5] J. MacNair and J.W. Jorgenson, presented at the 20th International Symposium on High Performance Liquid Phase Separations, San Francisco, CA, June 1996.
[6] F.D. Antia and Cs. Horváth, J. Chromatogr., 435 (1988) 1–15.
[7] H. Chen and Cs. Horváth, Anal. Methods Inst., 1 (1993) 213–222.
[8] R. Swart, J.C. Kraak and H. Poppe, J. Chromatogr. A, 670 (1994) 25–38.
[9] Y. Guo and L.A. Colon, Anal. Chem., 67 (1995) 2511–2516.
[10] J.H. Knox, Chromatographia, 26 (1988) 329.
[11] H. Yamamoto, J. Baumann and F. Erni, J. Chromatogr., 593 (1992) 313.
[12] H. Soni, T. Tsuda and M.V. Novotny, J. Chromatogr., 559 (1991) 547.
[13] S. Li and D.K. Lloyd, J. Chromatogr. A, 666 (1994) 321.
[14] F. Lelievre, C. Yan, R.N. Zare and P. Gareil, J. Chromatogr. A, 723 (1996) 145–156.
[15] S. Hjertén, J.-L. Liao and R. Zhang, J. Chromatogr., 473 (1989) 273–275.
[16] C. Fujimoto, J. Kino and H. Sawada, J. Chromatogr. A, 716 (1995) 107–113.
[17] F. Svec and J.M.J. Frechet, Anal. Chem., 64 (1992) 820–822.
[18] S. Hjertén, K. Nakazato, J. Mohammad and D. Eaker, Chromatographia, 37 (1993) 287–294.
[19] Q.C. Wang, F. Svec and J.M.J. Frechet, Anal. Chem., 65 (1993) 2243–2248.
[20] Y.-M. Li, J.-L. Liao, K. Nakazato, J. Mohammad, L. Terenius and S. Hjertén, Anal. Biochem., 223 (1994) 153–158.
[21] Q.C. Wang, F. Svec and J.M.J. Frechet, J. Chromatogr. A, 669 (1994) 230–235.
[22] S. Hjertén, D. Eaker, K. Elenbring, C. Ericson, K. Kubo, J.-L. Liao, C.-M. Zeng, P.-A. Lidstrom, C. Lindh, A. Palm, T. Srichiayo, L. Valtcheva and R. Zhang, Jpn. J. Electroph., 39 (1995) 105–118.
[23] J. Matsui, T. Kato, T. Takeuchi, M. Suzuki, K. Yokoyama, E. Tamiya and I. Karube, Anal. Chem., 65 (1993) 2223–2224.
[24] N. Tanaka, T. Ebata, K. Hashizume, K. Hosoya and M. Araki, J. Chromatogr., 475 (1989) 195–208.
[25] F. Nevejans and M. Verzele, J. Chromatogr., 406 (1987) 325–342.
[26] K. Nakanishi and N. Soga, J. Am. Ceram. Soc., 74 (1991) 2518–2530.
[27] K. Nakanishi and N. Soga, J. Non-Cryst. Solids, 139 (1992) 1–13 and 14–24.
[28] K. Nakanishi, H. Minakuchi, N. Soga and N. Tanaka, J. Sol-Gel Sci. Technol., in press.
[29] H. Minakuchi, K. Nakanishi, N. Soga, N. Ishizuka and N. Tanaka, Anal. Chem., 68 (1996) 3498–3501.
[30] N. Tanaka, H. Kinoshita, M. Araki and T. Tsuda, J. Chromatogr., 332 (1985) 57–69.
[31] J.H. Knox and H.P. Scott, J. Chromatogr., 316 (1984) 311–332.
[32] K.K. Unger, Porous Silica, Elsevier, Amsterdam, 1979, Ch. 5.
[33] L.K. Frevel and L.J. Kressley, Anal. Chem., 35 (1963) 1492–1502.
[34] K. Kimata, K. Iwaguchi, S. Onishi, K. Jinno, R. Eksteen, K. Hosoya, M. Araki and N. Tanaka, J. Chromatogr. Sci., 27 (1989) 721–728.
[35] J.C. Giddings, Dynamics of Chromatography, Marcel Dekker, New York, 1965.
[36] N. Tanaka, K. Kimata, Y. Mikawa, K. Hosoya, T. Araki, Y. Ohtsu, Y. Shiojima, R. Tsuboi and H. Tsuchiya, J. Chromatogr., 535 (1990) 13–31.
[37] L.R. Snyder and J.J. Kirkland, Introduction to Modern Liquid Chromatography, Wiley-Interscience, New York, 1979, Ch. 5.
[38] P.A. Bristow and J.H. Knox, Chromatographia, 10 (1977) 279–289.
[39] C.R. Wilke and P. Chang, Am. Inst. Chem. Engr. J., 1 (1955) 264.
[40] N.B. Afeyan, N.F. Gordon, I. Maszaroff, L. Varady, S.P. Fulton, Y.B. Yang and F.E. Regnier, J. Chromatogr., 519 (1990) 1–29.
[41] N.B. Afeyan, S.P. Fulton and F.E. Regnier, J. Chromatogr., 544 (1991) 267–279.
[42] L.J. Cole, N.M. Schultz and R.T. Kennedy, J. Microcol. Sep., 5 (1993) 433–439.
[43] H. Nagasawa, Y. Furuya, Y. Matsumoto and N. Oi, Chromatography, 14 (1993) 120–121.